World J. Surg. 24, 171–182, 2000
DOI: 10.1007/s002689910030

WORLD
Journal of
SURGERY

Adrenal Gland and Renal Sonography

Andrew F. Little, M.B.B.S., M.S.

Medical Imaging Department, St. Vincent's Hospital, 41 Victoria Parade, Fitzroy, Victoria 3065, Australia

Abstract. Ultrasound (US) is an established imaging modality for the assessment of the kidneys and adrenal glands. The advantages include its lack of ionizing radiation, speed, multiplanar real time evaluation, and cost compared with more expensive modalities. The addition of color Doppler also permits accurate evaluation of blood flow, which is especially useful in renal assessment. As with all sonography, both renal and adrenal US are highly dependent on the operator's skill and experience and require meticulous scanning techniques. In particular, adrenal sonography can be difficult due to the lack of a satisfactory acoustic window through which the incident US beam passes. This review summarizes the various morphologic appearances seen in common renal and adrenal pathologies, many of which have characteristic US appearances enabling accurate diagnosis.

Ultrasound (US) is an established modality for the assessment of the adrenal glands and kidneys. This article reviews the morphologic appearances seen in common adrenal and renal pathologies, many of which have characteristic US appearances enabling accurate diagnosis.

Adrenal Sonography

Although computed tomography (CT) is generally regarded as the best modality for adrenal gland evaluation, sonography has an important role to play in adrenal gland evaluation due to its speed, lack of ionizing radiation, and favorable cost. Adrenal sonography is frequently challenging due to the gland's position high in the abdomen in a location that is often obscured by intervening bowel gas. Therefore, an accurate and reproducible scanning technique is required for adequate evaluation.

Normal Adrenal Glands

The normal adrenal glands are situated in the eleventh to twelfth rib spaces adjacent and lateral to the L1 vertebral body. The glands measure approximately 3×6 cm and are 4 mm thick. Each gland consists of 3 portions comprising an anteromedial ridge with medial and lateral limbs. The 2 limbs encompass the upper pole of their respective kidneys. The glands are surrounded by a fibrous capsule.

The right adrenal gland is pyramidal in shape and is situated immediately posterior to the inferior vena cava. The gland lies adjacent to the crus of the diaphragm (which is a parallel medial relation to the medial limb of the gland) with the lateral limb of the gland adjacent to the posteromedial aspect of the liver.

The left adrenal gland is also positioned anteromedially to the kidney, but is more crescentic in shape compared with the right adrenal gland. The anteromedial ridge of the gland is more convex and the lateral and medial limbs are slightly shorter than the right. The gland lies lateral to the left crus of the diaphragm and has a posterior relation to the lesser sac and stomach superiorly and the pancreatic body and splenic vasculature caudally.

The medial limbs of both glands are larger superiorly and are smaller inferiorly where the lateral limbs are larger inferiorly and diminished in size superiorly. The glands are composed of cortex and medulla. The adrenal medulla secretes catecholamines where the adrenal cortex is divided into 3 distinct zones: the zona glomerulosa, which secretes aldosterone, and the zona fasciculata and zona reticularis, which secrete cortisol and androgens [1–4].

Scanning Techniques

With the advent of high-resolution scanning, the adrenal glands have become easier to examine, although as in all sonographic examinations, the success of visualization depends upon patient body habitus and operator skill and experience.

Adrenal gland visualization in a single plane is not possible due to its complex shape and therefore a multiplanar technique is required for all evaluations. Both glands are best assessed through an intercostal approach. The liver can be used as an acoustic window for evaluation of the right adrenal gland and the spleen can be used similarly as an acoustic window to evaluate the left adrenal gland.

On the right side, the transducer is placed approximately in the ninth to tenth intercostal spaces in the mid- to anterior axillary line with the probe scanning transversely and rotating the scan plane from the mid-portion of the kidney to above the kidney particularly situated posterior to the inferior vena cava. In this sequence, the anteromedial ridge and limbs can be identified with both limbs seen as an inverted Y. Coronal evaluation is then obtained by rotating the transducer 90 degrees from the transverse axis. Once the upper pole of the kidney is located, the transducer is angled medially to detect both limbs of the gland which again can be displayed simultaneously as an inverted Y- or V-shaped structure [5, 6].

The left adrenal gland is also best detected by scanning intercostally at approximately the ninth to tenth interspaces. However, the acoustic window through the spleen or kidney is often smaller than that obtained through the liver, rendering left adrenal gland

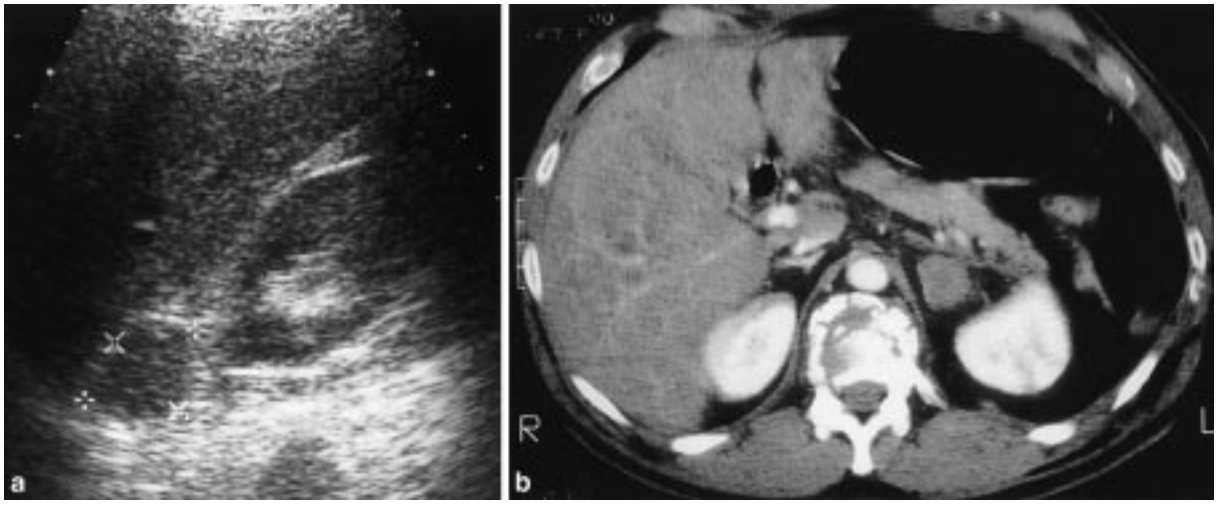

Fig. 1. Adrenal hemorrhage. **a.** Sagittal sonogram of the left upper quadrant after trauma in a 20-year-old man. The examination demonstrates a focal homogeneous adrenal gland mass consistent with either an adenoma or hemorrhage. **b.** Axial computed tomogram in the same patient demonstrates a burst fracture of the L3 vertebral body signifying severe trauma. In this clinical context, the adrenal mass is likely to represent a focal adrenal hemorrhage.

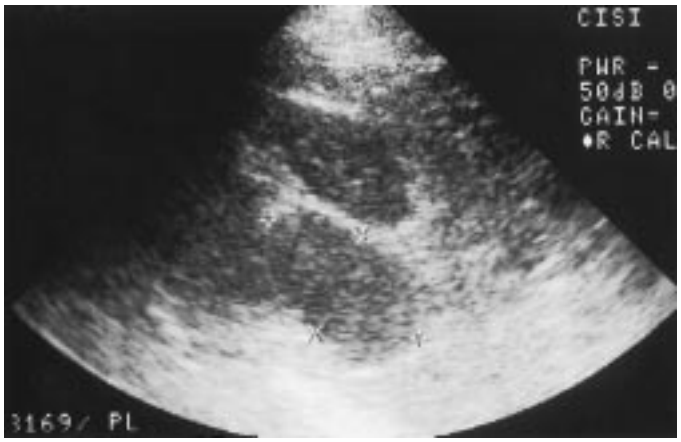

Fig. 2. Adrenal adenoma. Sagittal sonogram of the right adrenal gland demonstrating a small focal homogeneous mass found incidentally in a young patient with normal biochemistry. The size and homogeneity suggest a benign etiology. Depending on the clinical context, the lesion could be managed conservatively by routine follow-up.

detection more difficult. This can be further compromised by the presence of bowel gas within the stomach and adjacent jejunal loops. Both coronal and transverse scans should be performed with the upper pole of the kidney as a landmark from which to detect the adrenal gland, which can then be recognized as a characteristic V shape in the appropriate location. In some circumstances, right lateral decubitis and erect posture views may be required if left adrenal visualization is suboptimal [5, 6].

Structures that frequently simulate masses include adjacent lymphadenopathy, upper pole renal lesions, enlargement of the caudate lobe of the liver and accessory spleens or splenuculi, and gastric fundal abnormalities.

Adrenal Pathology

Adrenal Cysts. These can occur at any age but are detected most commonly in the 3rd to 5th decades. They are usually asymptomatic and found incidentally, but with an increase in size may present with vague abdominal pain. The cysts are most commonly endothelial in origin but also may develop after resolution of previous adrenal gland hemorrhage. They are frequently round with a smooth imperceptible wall with prominent through-transmission and posterior acoustic enhancement. Infrequently there is internal septation and rarely the cyst wall also may calcify. Because of their benign nature, adrenal cysts can be imaged serially for follow-up, but if symptomatic can be aspirated percutaneously [7].

Adrenal Hemorrhage. This may be spontaneous and associated with severe stress, thrombocytopenia, or a complication of anticoagulation or be posttraumatic from severe thoracic, abdominal, or retroperitoneal trauma due to direct compression or rapid deceleration.

Sonographically, acute hemorrhage is represented by an echogenic mass within the adrenal parenchyma which rapidly becomes isoechoic and then anechoic over time (Fig. 1a,b). The hematoma may eventually completely resolve, develop into an adrenal cyst, or calcify. While unilateral adrenal hemorrhage has relatively few clinical sequelae, bilateral hemorrhages may result in an increased risk of adrenal insufficiency [8, 9].

Benign Adrenal Tumors. ADENOMA. Most cortical adenomas are approximately 1–2 cm in diameter and are nonfunctioning. The incidence is up to 2% of adult autopsies and approximately 10% of patients will have bilateral adrenal adenomas.

Patients presenting with hyperfunctioning adrenal adenomas present with symptoms of excess hormone secretion compared with the nonhyperfunctioning adenomas. Hyperfunctioning renal adenomas resulting in Cushing's syndrome are due to excessive cortisol excretion with Conn's syndrome resulting from excess aldosterone secretion. Patients with small adrenal masses and clinical evidence of excess hormone production require further investigation and ultimately surgery.

Adrenal masses with no clinical evidence of hyperfunctioning adrenal hormone secretion are managed usually on size criteria alone. Lesions approximately 1–2 cm in size are considered benign

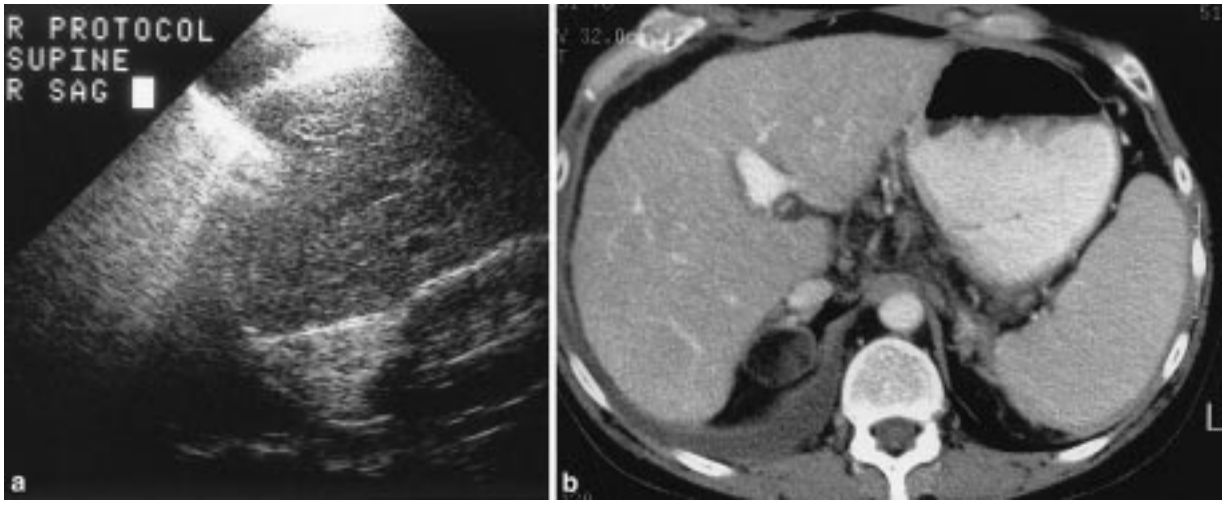

Fig. 3. Adrenal myelolipoma. **a.** Sagittal sonogram of the right upper quadrant demonstrating an enlarged, diffusely echogenic right adrenal gland. **b.** Axial computed tomogram demonstrates the fat content of the mass, confirming the lesion to be a myelolipoma.

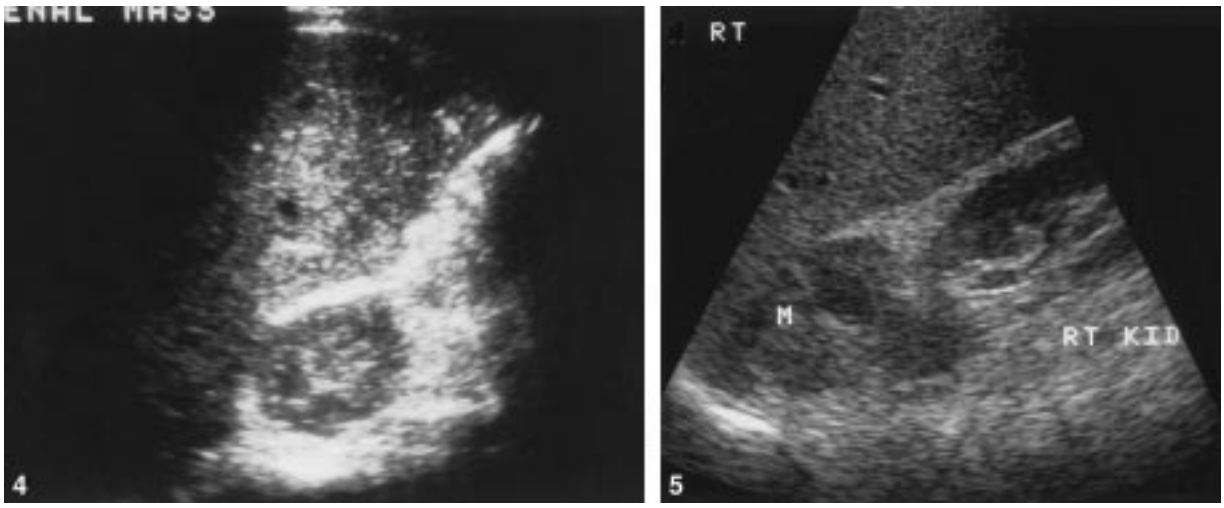

Fig. 4. Adrenal pheochromocytoma. Transverse sonogram of the right upper quadrant demonstrating a moderate-sized heterogeneous adrenal mass of mixed echogenicity in a patient presenting with hypertension and elevated catecholamine levels.

Fig. 5. Adrenal metastasis. Sagittal sonogram of the right upper quadrant demonstrating biopsy-proven adrenal metastasis characterized by an enlarged heterogeneous adrenal mass in a patient with documented primary bronchogenic malignancy.

and are routinely followed up. Lesions approximately 3–6 cm in size need to be regarded as potentially malignant and managed accordingly following needle biopsy. Sonographically, adrenal adenomas are round, solid, and homogeneous (Fig. 2). It is important to accurately determine the site of these lesions and not confuse an incidentally discovered adrenal adenoma from an upper pole renal mass which may have implications of malignancy [2, 3].

MYELOLIPOMA. These lesions are usually discovered incidentally and are benign nonhyperfunctioning tumors consisting of varying amounts of fat and bone marrow elements. Most of these lesions are <5 cm in diameter. Sonographically, myelolipomas are echogenic masses if they predominantly contain fat, but if there is a greater proportion of myeloid material, the tumors may be more isoechoic or hypoechoic. Accurate localization of these echogenic masses to the adrenal gland is important as the differential diagnosis includes renal angiomyelolipoma or retroperitoneal liposarcoma or teratoma (Fig. 3a,b) [10, 11].

PHEOCHROMOCYTOMA. These tumors are usually hyperfunctioning and secrete adrenaline and noradrenaline. The clinical presentation includes episodic hypertension, headaches, and palpitations. The majority of pheochromocytomas arise within the adrenal medulla but approximately 10% can arise in extraadrenal sites of autonomic nervous tissue. The majority of these lesions are benign but approximately 10% are malignant and 10% may be multiple. Multiple lesions are most often associated with Sipple's syndrome or Von Hippel-Lindau syndrome. The diagnosis is most often confirmed biochemically by measuring urine catecholamine levels. The sonographic presentation of a small pheochromocytoma is of a well-defined round mass of uniform low echogenicity. However, when large, the lesions can become necrotic or hemorrhagic and may present with increasing heterogeneity (Fig. 4) [12].

Malignant Adrenal Neoplasms. ADRENAL CORTICAL CARCINOMA. Primary adrenal cortical carcinoma is a rare malignancy and in adults is frequently nonhyperfunctioning, whereas in children the tumors are most often hyperfunctioning resulting in hyperadrenal syndromes. Hyperfunctioning tumors are detected earlier and can present with Cushing's syndrome, adrenogenital syndrome, precocious puberty, and rarely Conn's syndrome. If hyperfunctioning, the masses have frequently invaded the renal vein or inferior vena cava (IVC) on presentation and blood-borne and nodal metastases are not uncommon.

The sonographic appearance of adrenal cortical cancer depends upon its size at presentation. The small hyperfunctioning tumors are usually homogeneous and hypoechoic. The larger nonhyperfunctioning lesions are usually more heterogeneous, often with central areas of necrosis and hemorrhage [13].

LYMPHOMA. Primary adrenal gland lymphoma is rare, but adrenal gland involvement can occur due to contiguous spread from associated retroperitoneal adenopathy. The sonographic appearance of lymphoma is usually associated with discrete retroperitoneal lymphadenopathy [14, 15].

ACQUIRED IMMUNODEFICIENCY SYNDROME (AIDS). Focal adrenal gland masses in patients with AIDS may be related to infection or neoplasm. Infections are most likely of the opportunistic variety such as cytomegalovirus (CMV), candida, cryptococcus, toxoplasmosis, *Mycobacterium avium* intracellulare (MAI), or herpes. Neoplasms may be either primary lymphoma or Kaposi's sarcoma. Sonographic appearances demonstrate a nonspecific solid mass within the adrenal gland which may have associated necrosis if large.

METASTASES. The adrenal gland is a common site for metastatic disease primarily arising from the lung, breast, melanoma, kidney, thyroid, and colon. Most lesions are discovered incidentally during the workup of patients with a known primary malignancy. Although an adrenal lesion is still more likely to be an adenoma, the staging of the patient's malignancy requires adrenal assessment. If the lesions are small and relatively homogeneous, the most likely diagnosis is adenoma. If the lesions are larger with associated hemorrhage or necrosis, they most likely represent metastases. The sonographic appearance of metastases largely depends upon the size of the lesion within the adrenal gland, with larger lesions being more heterogeneous due to associated necrosis and hemorrhage (Fig. 5) [16, 17].

Renal Sonography

Renal sonography is an expeditious imaging modality for rapidly and accurately evaluating renal pathology. The position of the kidneys in the upper abdomen usually permits adequate assessment of renal parenchyma and renal morphology especially when using the liver and spleen as acoustic windows. Color-enhanced duplex Doppler evaluation of the renal vasculature also allows a noninvasive assessment of the renal vasculature.

Normal Kidneys

Both kidneys lie within the retroperitoneal space high in the abdomen immediately adjacent to the upper lumbar vertebrae with the medial margins of the kidneys laying on the lateral edge of the psoas muscles. Due to the presence of the liver, the right kidney often lies in a lower position compared with the left kidney. The long axes of both kidneys usually run parallel to the lateral margin of the psoas muscles and therefore the longitudinal axes run from a medial to a lateral position. Furthermore, the kidneys are rotated slightly anteriorly such that the renal hilum usually lies in the most superior aspect of the kidney. The right kidney is related anteriorly to the adrenal gland, liver, hepatic flexure of the colon, and second part of the duodenum. The left kidney is related anteriorly to the spleen, adrenal gland, pancreatic tail, and splenic flexure of the colon. Both kidneys are bordered by the anterior and posterior renal fascias and are surrounded within this perirenal space by a large amount of retroperitoneal fat. Both the anterior and posterior renal fascias separate the perirenal space from the anterior and posterior pararenal spaces. These fascial delineations explain the appearance of renal pathology and related fluid collections [1, 18, 19].

The adult kidneys measure approximately 11 cm in their long axes and usually approximately 5 cm in width. However, renal size is related to the sex, age, and body habitus of the patient and renal lengths can vary significantly from approximately 7 to 15 cm [19]. The sinus of the kidney contains the arterial supply and venous drainage and collecting systems. The renal parenchyma is composed of cortex and medulla. The renal medulla is in the form of medullary pyramids that project into the collecting system calyces, which then coalesce to form the renal pelvis and ureter. The pyramids are usually hypoechoic with respect to the adjacent renal cortex. The normal renal cortex is usually of lower echogenicity than the surrounding adjacent hepatic or splenic echotexture. The renal sinus is of increased echogenicity due to contained fat (Fig. 6) [20, 21].

Scanning Techniques

As with all sonographic examinations, operator skill and experience and patient body habitus are important aspects in the success of renal sonography. However, the renal position with adjacent hepatic and splenic acoustic windows usually allows satisfactory evaluation, although the left kidney may be more difficult to visualize due to artifact from jejunal bowel loops and the splenic flexure. Therefore, patients frequently need to be scanned in various postures. The most successful positions for satisfactory renal sonography are the supine, oblique, and lateral decubitus postures utilizing a combination of subcostal and intercostal approaches and using the spleen and liver as acoustic windows. The posterior prone approach is usually unsatisfactory due to the paraspinal musculature resulting in poor renal visualization.

Scanning technique requires accurate determination of renal length and width and assessment of cortical thickness. Renal length in particular is an important indicator of normality and it is important that an accurate measurement is obtained in the longest length of the longitudinal axis without artifactual foreshortening [22].

If a normal kidney is not visualized within the renal fossa, a systematic search should be made within the retroperitoneum and pelvis for a contralateral or pelvic kidney or to exclude a crossed fused ectopia. The appearances of fetal lobulation, splenic humps, and hypertrophied renal septa are frequent normal variations. Hypertrophied columns of Bertin, however, can be confused with a focal malignancy. These are differentiated from renal tumors as usually the renal outline is not abnormal compared with a focal

mass lesion. In addition, the echogenicity of the hypertrophied septa is similar to the adjacent cortex. If further confirmation of a prominent septa of Bertin is required, a nuclear scintigraphic or computed tomographic (CT) scan is usually diagnostic.

Renal Pathology

Renal Cysts and Renal Cystic Disease. SIMPLE RENAL CYSTS. Renal cysts are divided into simple and complex with cystic renal disease encompassing those inherited conditions such as adult polycystic disease, Von Hippel-Lindau disease, tuberous sclerosis, and medullary cystic disease.

Simple renal cysts are the most common renal lesion evaluated sonographically and are usually an incidental finding during a sonographic evaluation of the upper abdominal viscera. The cysts are usually single and rarely symptomatic unless hemorrhage or infection has complicated the cyst. The sonographic features are of a sharply defined and imperceptible wall, absent internal echoes, or septation with prominent posterior acoustic enhancement (Fig. 7). Although simple renal cysts with the above features are rarely of clinical concern, if there are findings of increased echoes with associated septa and thickened walls or calcification, further investigation of these cysts may be warranted to exclude malignancy (Figs. 8, 9) [23]. Most simple renal cysts arise in the renal cortex, but multiple cysts may arise within the renal sinus resulting in parapelvic cysts [24].

MULTICYSTIC DYSPLASTIC KIDNEY. This condition is developmental and is characterized by an abnormal collection of cysts with little or no renal parenchyma. The condition is usually unilateral and related to in utero renal tract obstruction. It may be associated frequently with contralateral pelviureteric junction (PUJ) obstruction (Fig. 10) [25].

END-STAGE RENAL DISEASE. Acquired renal cystic disease in dialysis patients is a bilateral disorder occurring in end-stage kidneys and is seen in up to 90% of patients treated with dialysis for 10 years or more. The condition is usually of limited clinical significance, although intracystic and perinephric hemorrhage, cystic infection, renal calculi, and small renal neoplasms may be associated (Fig. 11) [26].

CYSTIC RENAL DISEASE. These conditions are commonly of hereditary origin with the most common condition being polycystic renal disease [27]:

Adult polycystic renal disease is inherited as an autosomal dominant condition and if not discovered early presents in middle age with hypertension, hematuria, and an abdominal mass. The condition is associated in approximately one third of patients with other visceral manifestations such as hepatic, pancreatic, and splenic cysts and less frequently cysts involving the epididymis, seminal vesicles, uterus, and thyroid.

The earliest sonographic presentation is of increased renal echogenicity due to numerous small cysts that are imperceptible in the early stage. This may be associated with mild renal enlargement and loss of corticomedullary differentiation. Later in the typical presentation of the condition, both kidneys are enlarged with marked distortion of the renal architecture and disruption of the normal corticomedullary differentiation and renal sinus echogenicity with extensive cysts of varying size and complexity (Fig. 12). Many cysts may be complicated by associated hemorrhage or infection resulting in abdominal pain. However, it is often difficult to document accurately the specific cyst involved in the patient's clinical symptoms so that guided renal cyst aspiration may not always be feasible.

Von Hippel-Lindau disease is a congenital disease that is inherited as an autosomal dominant condition and is characterized by the presence of multiple renal cysts, adenomas, and angiomas; less commonly, renal adenocarcinomas and hemangioblastomas also may be associated with this condition. It is a multisystem disorder also affecting the central and peripheral nervous systems, pancreas, and adrenal glands [28, 29].

Tuberous sclerosis is a multisystem disorder affecting the central nervous system, skin, skeleton, lungs, and heart, and the renal manifestations are those of multiple angiomyelolipomas and renal cysts [30].

Medullary cystic disease is inherited as an autosomal dominant condition with sonographic features of small kidneys of increased echogenicity due to numerous small medullary cysts [31].

Benign Renal Neoplasms. ADENOMA. The sonographic features of renal adenomas are nonspecific and generally inseparable from those of malignant lesions.

ONCOCYTOMA. This benign lesion often presents later in life as a large renal mass that presents with associated pain or bleeding. While oncocytoma has a characteristic angiographic appearance and sonographically may have a stellate central scar, the features are usually nonspecific and further investigation is usually required [32].

ANGIOMYELOLIPOMA. This benign hematoma is composed of adipose tissue, angiomatous tissue, and smooth muscle. It is most often visualized in middle-aged women, but a small proportion of these lesions are associated with the inherited condition of tuberous sclerosis. The lesions most often present following a complication such as hemorrhage which occurs as a result of fragile and immature blood vessels. The adipose component of the lesion results in characteristic sonographic findings of a markedly echogenic, well-defined focal lesion within the renal cortex (Fig. 13) [33].

MULTILOCULATED CYSTIC NEPHROMA. This is a rare benign tumor that presents in the pediatric population and consists of multiple cysts with associated fibrous tissue. Sonographically, the features are relatively nonspecific and often are indistinguishable from cystic adenocarcinoma [34].

Malignant Renal Neoplasms. RENAL CELL CARCINOMA. This is the most common solid renal neoplasm and usually presents in middle age, being more common in men than in women. There are a number of renal conditions that have an increased risk of developing renal cell carcinoma such as Von Hippel-Lindau disease, tuberous sclerosis, polycystic kidneys, and dialysis-related acquired renal cystic disease.

The sonographic appearance of renal cell carcinoma is usually that of a solid mass of mixed echogenicity occupying a portion of the renal substance. The tumor may be isoechoic, hypoechoic, or echogenic, although the majority are usually isoechoic to the adjacent parenchyma (Fig. 14). Approximately 10% have associated calcification and cystic or necrotic change also may be evi-

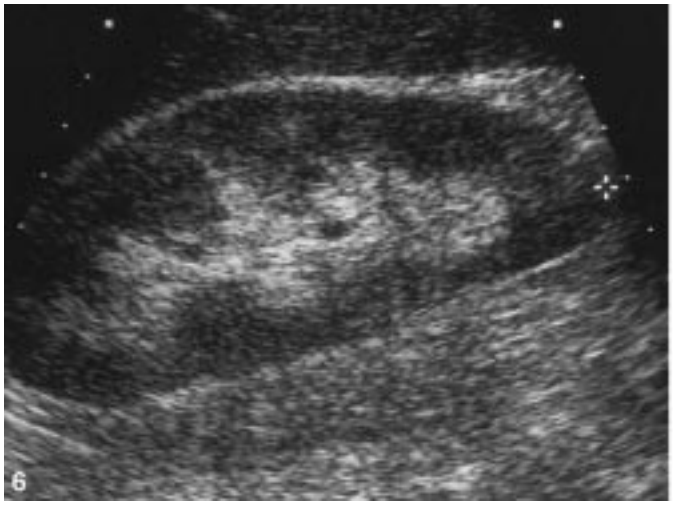

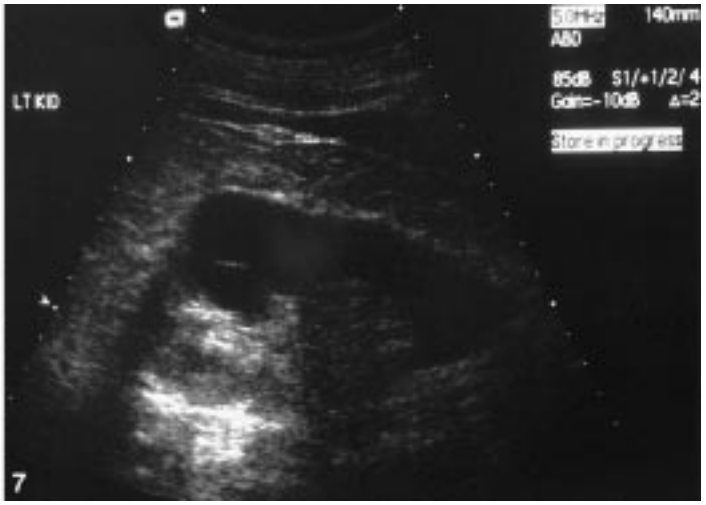

Fig. 6. Normal kidney. Sagittal sonogram of the right kidney demonstrating normal parenchymal and renal sinus echotexture and normal cortical thickness.

Fig. 7. Simple renal cyst. Sagittal sonogram of 2 adjacent simple renal cortical cysts occupying the mid and upper pole regions of the left kidney. Note the imperceptible walls, prominent posterior acoustic enhancement, and lack of echoes within the cyst.

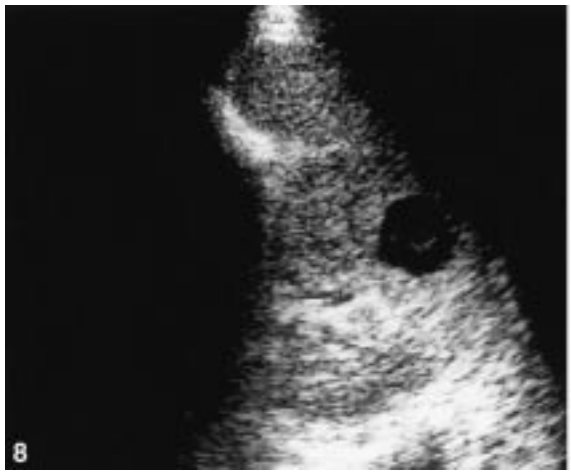

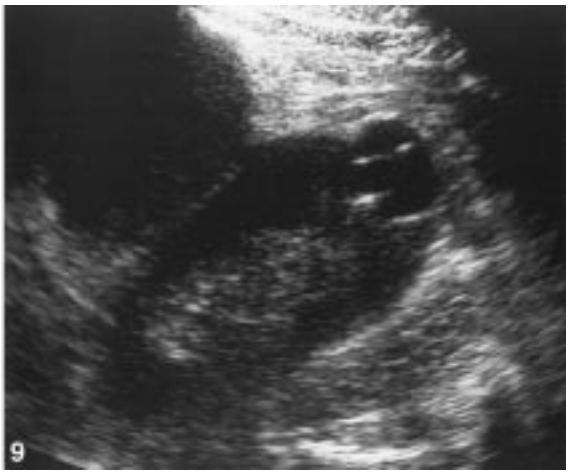

Fig. 8. Renal cyst. Sagittal sonogram of a renal cyst with a solitary septation. Note the well-defined margins and posterior acoustic enhancement typical of a cyst. The presence of the septation indicates this is not a simple cyst and should be followed up.

Fig. 9. Complex renal cyst. Sagittal sonogram of a multiseptated renal cyst with thickened septations, some portions of which are calcified. Further imaging investigation is required to exclude a cystic renal cell carcinoma.

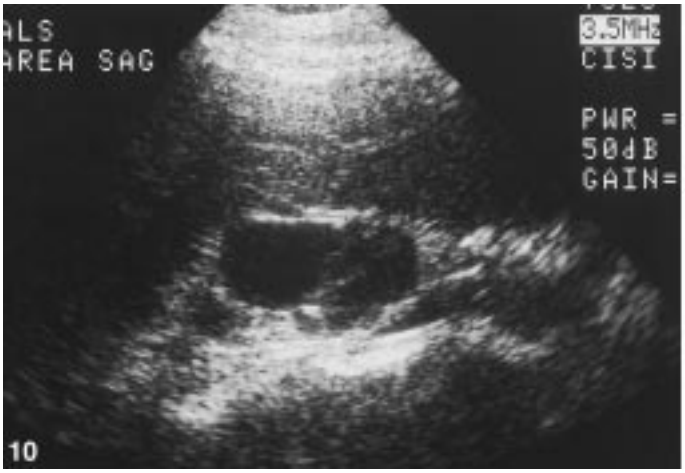

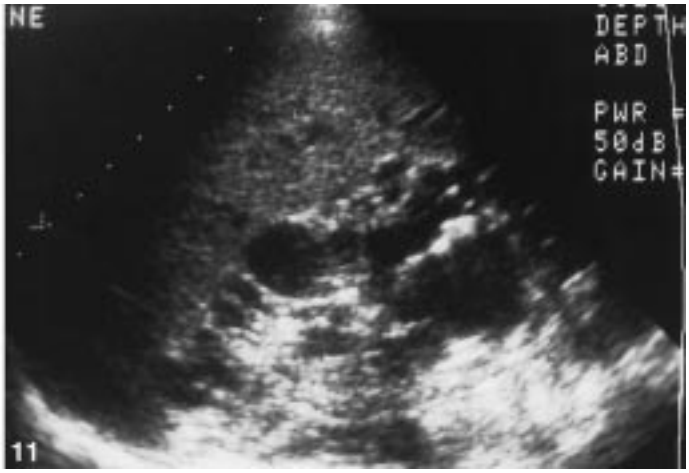

Fig. 10. Multicystic dysplastic kidney. Sagittal sonogram of irregular multiple noncommunicating renal cysts with absent renal parenchyma.

Fig. 11. Acquired dialysis end-stage renal disease. Sagittal sonogram of end-stage dialysis kidneys demonstrating multiple intrarenal cysts and absent renal parenchyma.

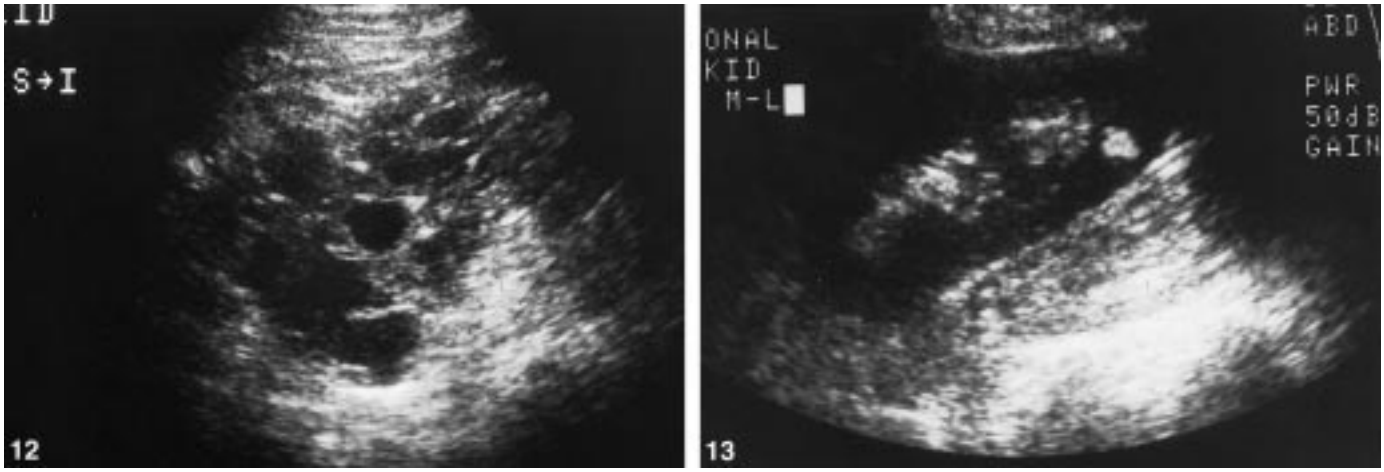

Fig. 12. Autosomal dominant polycystic kidney. Axial sonogram of the right kidney demonstrating numerous cysts distorting the renal contour in a patient with autosomal dominant polycystic renal disease.

Fig. 13. Angiomyelolipoma. Sagittal sonogram of the left kidney demonstrating a small focal echogenic lesion within the lower pole cortex. Computed tomographic scan confirmed the lesion to be of fat density.

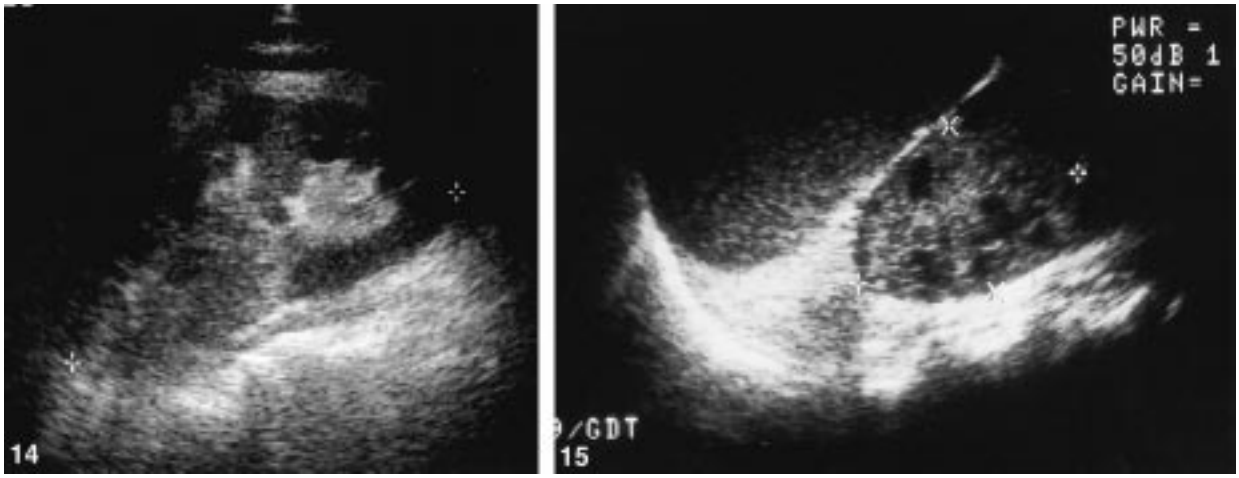

Fig. 14. Renal cell carcinoma. Sagittal sonogram of relatively isoechoic mass arising from the upper pole of the right kidney. The renal contour is not distorted significantly.

Fig. 15. Renal cell carcinoma. Sagittal sonogram of isoechoic mass arising from the upper pole of the right kidney with associated multifocal cystic change.

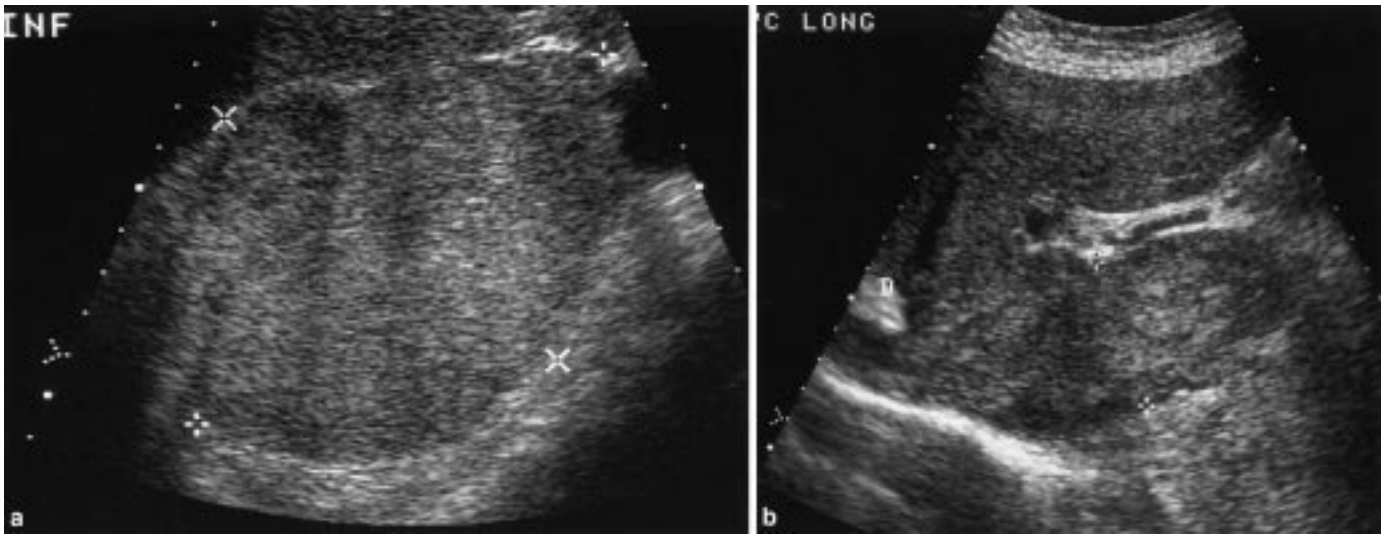

Fig. 16. Renal cell carcinoma and inferior vena cava invasion. **a.** Transverse sonogram of large isoechoic renal cell carcinoma. **b.** Sagittal sonogram demonstrating expansion and malignant invasion of adjacent inferior vena cava. D: diaphragm.

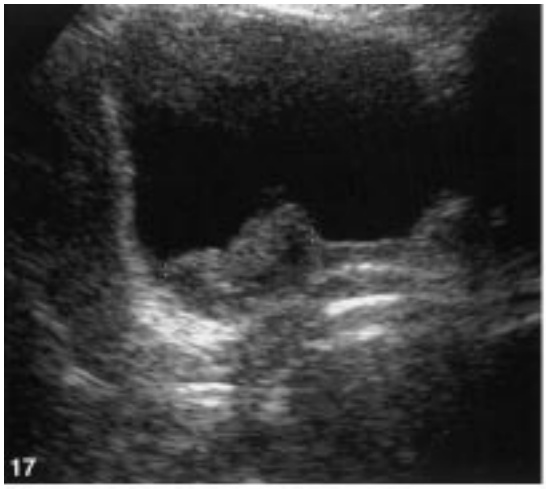

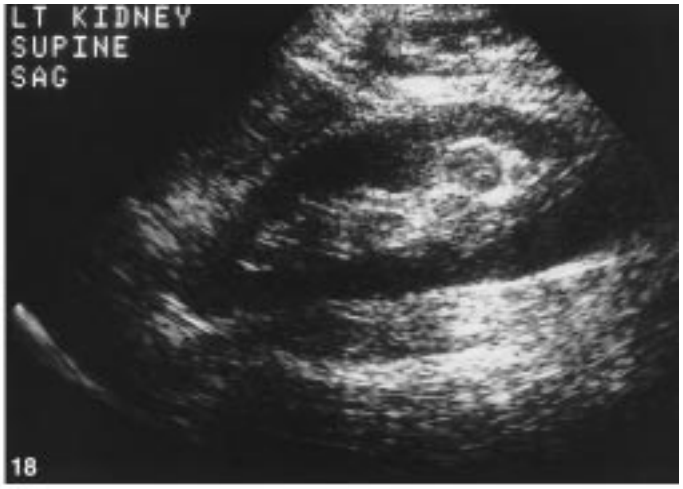

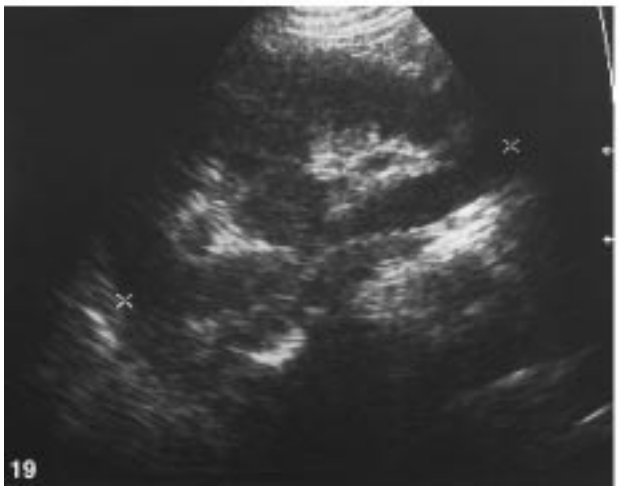

Fig. 17. Bladder transitional cell carcinoma. Transverse sonogram of bladder transitional cell carcinoma showing excellent visualization due to the surrounding urine.

Fig. 18. Renal transitional cell carcinoma. Sagittal sonogram of focal relatively isoechoic transitional cell carcinoma within the lower pole moiety of the renal collecting system.

Fig. 19. Lymphoma. Sagittal sonogram of focal biopsy-proven isoechoic lymphoma within the mid-pole of the right kidney. In a different clinical context, the appearances might be consistent with a hypertrophied column of Bertin. Differentiation between these 2 entities would require nuclear scintigraphy.

dent (Fig. 15). The lesions are usually hypervascular and therefore increased blood flow can be assessed with color duplex evaluation [35]. Color duplex evaluation of the renal vein and IVC is also useful to exclude venous invasion (Fig. 16a,b) [36, 37]. The presence of metastatic disease and lymphadenopathy is not always identified sonographically and therefore CT is usually preferred in staging patients with suspected renal cell carcinoma [38].

TRANSITIONAL CELL NEOPLASMS. Transitional cell carcinomas (TCCs) most commonly involve the bladder and to a lesser extent the renal pelvis and ureter. Bladder TCCs that involve the trigone with resultant ipsilateral renal tract obstruction are often well-visualized sonographically (Fig. 17). TCCs are most often hypoechoic lesions and, depending upon the gain settings of the US machine, may be very difficult to detect accurately especially if small within an undilated pelvicalyceal collecting system (Fig. 18). CT is most useful for the evaluation of local and distant tumor spread and lymphadenopathy [39].

LYMPHOMA. Lymphomatous involvement of the kidney is usually a manifestation of diffuse multisystem non-Hodgkin's lymphoma. Primary renal lymphoma is uncommon. Sonographically, renal lymphoma usually presents as a solitary renal mass, with a smaller percentage presenting with multiple small masses or diffuse parenchymal infiltration. The lesions are usually hypoechoic and rarely echogenic (Fig. 19) [40].

METASTASES. Metastatic renal disease is not uncommon due to the high renal blood flow and therefore the common causes of metastatic disease are hematogenous in origin. Conditions such as lung, breast, renal cell carcinoma of the contralateral kidney, and gastrointestinal malignancies can metastasize to the renal parenchyma. The sonographic appearance depends on the morphology of the metastatic disease and may be a large focal solitary mass, multiple masses, or diffuse infiltration. Metastatic disease is usually hypoechoic and although the imaging features are nonspecific, in the appropriate clinical context metastatic disease needs to be considered [41].

Infections. ACUTE PYELONEPHRITIS. The sonographic evaluation of a patient with acute uncomplicated pyelonephritis often reveals normal appearances. When abnormal, the imaging findings are those of renal enlargement due to edema, altered echotexture which may become hypoechoic or echogenic, and loss of corticomedullary differentiation.

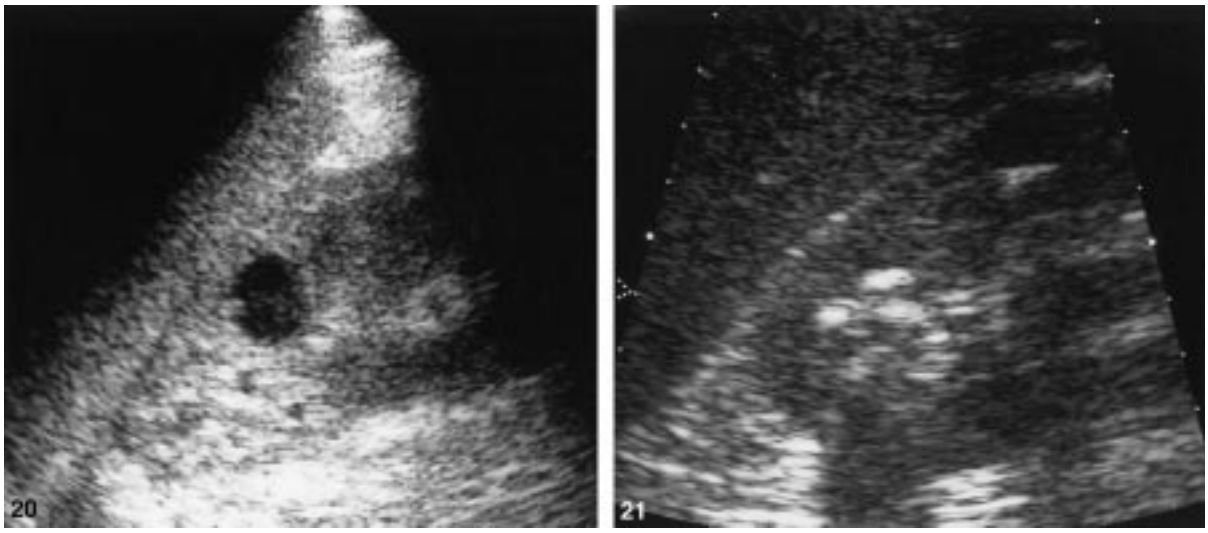

Fig. 20. Renal abscess. Sagittal sonogram of the right kidney demonstrating a focal hypoechoic lesion with contained debris consistent with a renal abscess. Needle aspiration confirmed renal abscess, which responded rapidly to appropriate antibiotics.

Fig. 21. Renal abscess. Sagittal sonogram of the right kidney demonstrating a focal ill-defined area of irregular echogenicity consistent with a gas-containing renal abscess.

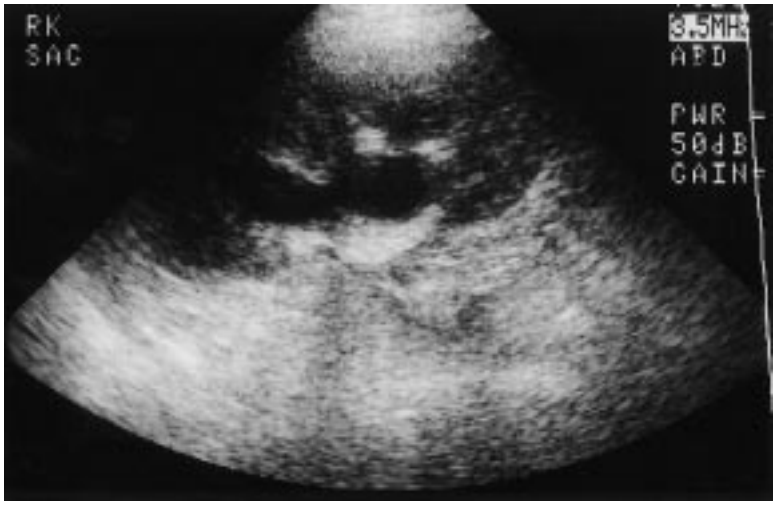

Fig. 22. Pyonephrosis. Sagittal sonogram of the right kidney demonstrating moderate hydronephrosis with associated contained echogenic debris consistent with pyonephrosis.

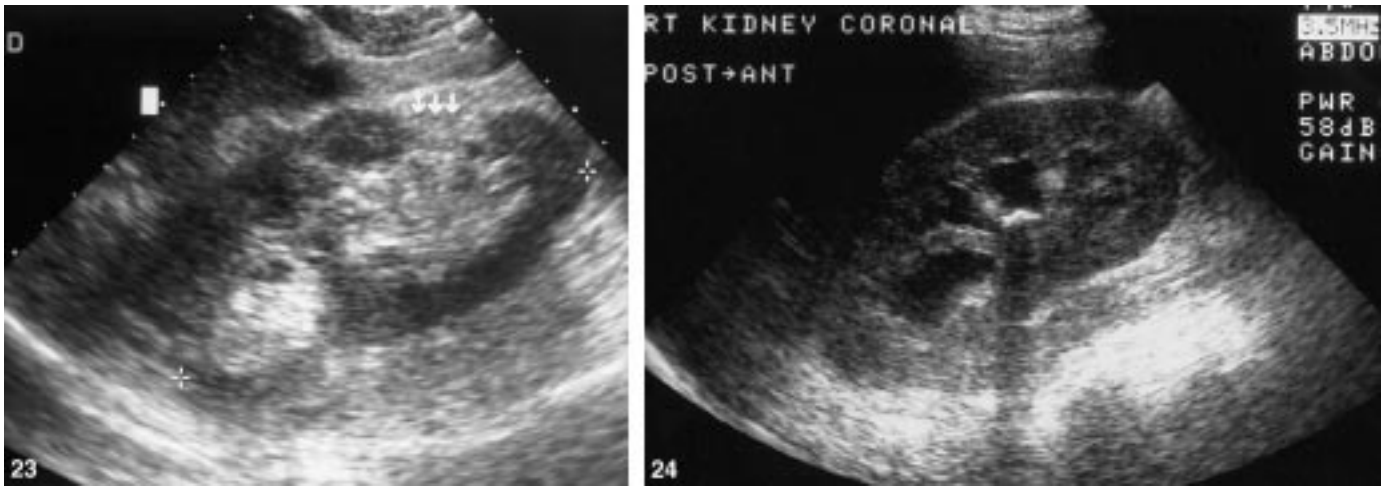

Fig. 23. Chronic pyelonephritis. Sagittal sonogram of the left kidney demonstrating a small kidney with associated focal cortical scarring (arrows) consistent with pyelonephritis.

Fig. 24. Renal calculus. Right renal ultrasound demonstrating moderate hydronephrosis and focal echogenic calculus with associated posterior acoustic shadowing.

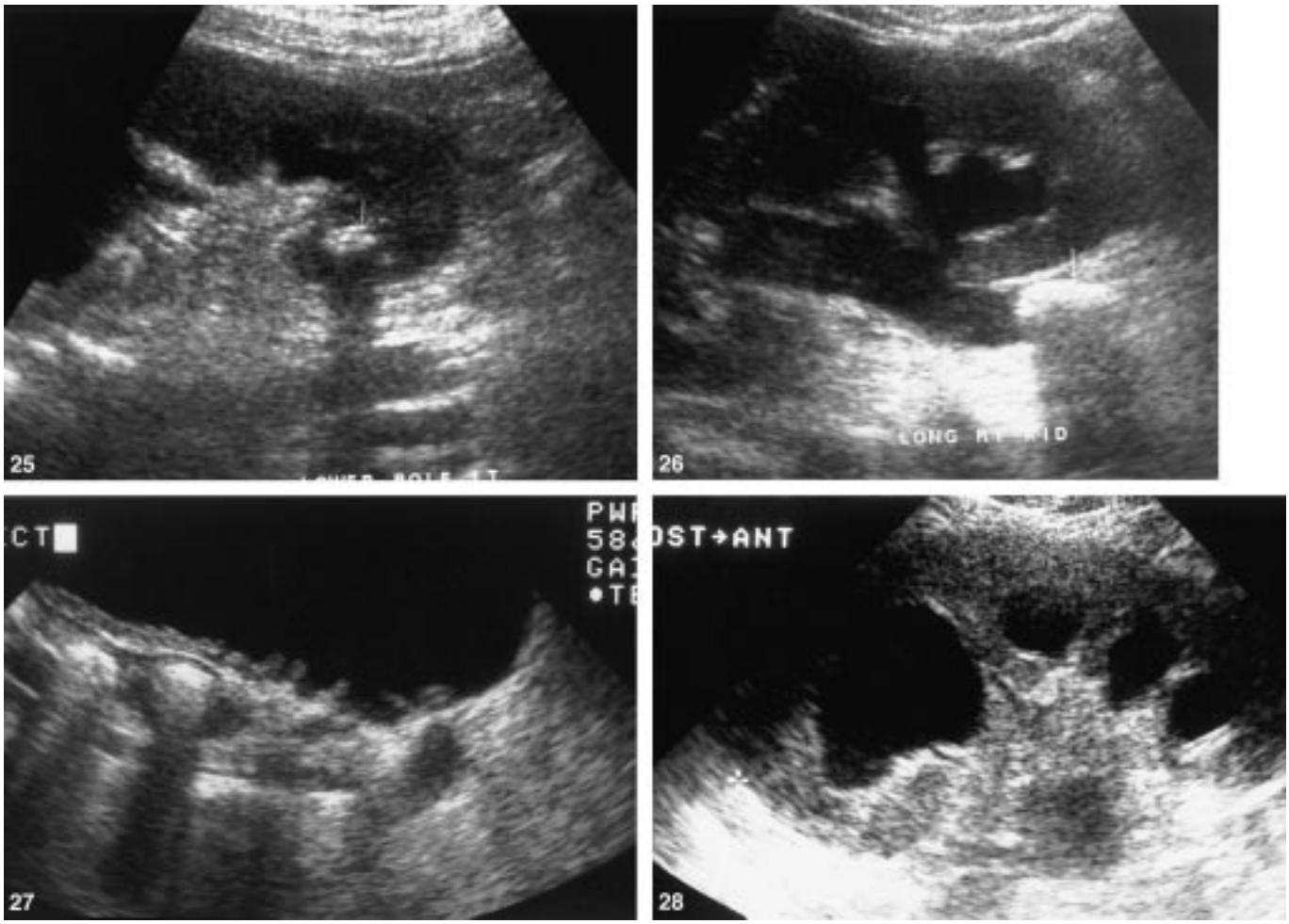

Fig. 25. Renal calculus. Sagittal sonogram of the left kidney demonstrating solitary lower pole moiety collecting system calculus with associated posterior acoustic shadowing (arrow).

Fig. 26. Ureteric calculus. Sagittal sonogram of the right kidney demonstrating obstructing calculus within the proximal ureter (arrow).

Fig. 27. Ureteric calculus. Sagittal sonogram of the bladder demonstrating obstructing calculi within the distal ureter.

Fig. 28. Hydronephrosis. Sagittal sonogram of the right kidney demonstrating marked pelvicalyceal collecting system dilatation due to distal obstructing calculus.

FOCAL PYELONEPHRITIS AND RENAL AND PERIRENAL ABSCESSES. The development of focal pyelonephritis is the early stage of renal suppuration. Previously this entity has been known by various names such as focal lobar nephronia or acute bacterial nephritis. The sonographic appearances of focal pyelonephritis are subtle and are usually those of an ill-defined hypoechoic area with associated increased colorflow on duplex imaging. As focal pyelonephritis progresses to a renal abscess, the sonographic appearances are more distinct characterized by a focal hypoechoic complex mass, sometimes with associated echogenic debris consistent with gas or necrosis (Figs. 20, 21). In addition, there is diminished or absent colorflow within the center of the lesion, but often with rim enhancement on color evaluation. If untreated, the continuation of renal infection can progress to perinephric abscess, which is due to perforation of the inflammatory lesion into the perinephric space. Sonographically, these fluid collections are hypoechoic, but the presence of gas or other debris can result in heterogeneous echogenicity [42, 43].

PYONEPHROSIS. This condition occurs due to renal obstruction and suppurative infection resulting in purulent material within the collecting system. The sonographic appearances demonstrate hydronephrosis and hydroureter depending on the level of obstruction. The presence of debris within the collecting system in these circumstances should raise the possibility of associated infection (Fig. 22).

CHRONIC PYELONEPHRITIS. This is an end-stage nephritis due to prolonged vesicoureteric reflux and multiple infections. This results in multiple focal scars or diffuse cortical scarring and the end stage is a small irregular kidney. The appearances may be unilateral or bilateral and are usually asymmetric. The sonographic appearances are predominantly those of renal cortex scarring adjacent to the renal pyramids (Fig. 23). This should be compared with renal fetal lobulation in which the cortical indentation appears between the medullary pyramids.

XANTHOGRANULOMATOUS PYELONEPHRITIS. This condition is a chronic suppurative infection associated with calculi and renal obstruction with a typical histologic appearance of lipid-laden macrophages. The disease presents most often in middle-aged women. The sonographic appearance is that of renal enlargement with multiple calculi resulting in associated acoustic shadowing and dilated calyces [44].

Renal Collecting System. CALCULI. Renal calculi usually are well-visualized sonographically and are characterized by discrete echogenic foci with associated posterior acoustic shadowing (Figs. 24, 25). The presence of shadowing is an important discriminating factor so that calculi and other echogenic foci such as fat can be differentiated. Vascular calcification within the renal sinus also can mimic calculi. Calculi can be detected within the urinary tract if there is associated obstruction (Figs. 26, 27) [45]. The mid-ureter is usually not well visualized due to intervening bowel gas and therefore calculi are often not detected in this location. Furthermore, ureteric calculi are seen rarely in an undilated ureter.

HYDRONEPHROSIS. Dilatation of the pelvicalyceal collecting system is known as hydronephrosis (Fig. 28) and is due usually to urinary tract obstruction, although there are other causes of hydronephrosis not due to obstruction. Reflux nephropathy is the major differential diagnosis of hydronephrosis not due to obstruction, with less frequent causes including postobstructive dilatation, increased urine production, and a prominent distensible pelvicalyceal collecting system. Although most cases of obstruction of the collecting system result in hydronephrosis, there are a few instances in which obstruction is present without hydronephrosis. This is seen most often in rupture of the collecting system after obstruction with resultant decompression into the surrounding perinephric space or in situations in which there is tumor invading the collecting system [46].

Résumé

L'échographie est bien reconnue comme une modalité d'imagerie pour évaluer les reins et les surrénales. Les avantages sont l'absence de radiation ionisante, sa rapidité et ses possibilités d'exploration dans tous les plans. En plus elle fonctionne en temps réel et ses coûts sont moindres par rapport à d'autres modalités d'imagerie. L'addition de la couleur permet l'évaluation précise du débit sanguin qui est surtout utile dans l'évaluation du rein. Comme avec toute échographie, l'évaluation du rein et de la surrénale est hautement dépendant de la compétence et de l'expérience des opérateurs, et demande des techniques manuelles méticuleuses. L'échographie de la surrénale est particulièrement difficile en raison de l'absence d'une fenêtre acoustique dans laquelle doivent passer les ondes ultrasoniques. Cette revue résume les aspects morphologiques rencontrés dans les pathologies rénales et surrénaliennes, qui pour plusieurs d'entre elles, ont des aspects caractéristiques permettant des diagnostiques précis.

Resumen

La ultrasonografía es una modalidad para generar imágenes diagnósticas útiles en la evaluación de los riñones y las glándulas suprarrenales. Sus ventajas incluyen la ausencia de irradiación ionizante, la velocidad, la posibilidad de visualización multiplanar en tiempo real, y su costo en comparación con otros métodos. La incorporación del Doppler a color permite la evaluación muy precisa del flujo sanguíneo, lo cual es particularmente útil en la evaluación renal. Como ocurre con todo tipo de sonografía, la ultrasonografía renal y suprarrenal es altamente dependiente de la habilidad y experiencia del operador y requiere una meticulosa técnica de escanografía. En particular, la sonografía suprarrenal puede ser difícil por razón de la ausencia de una ventana acústica satisfactoria que permita el paso al haz de ultrasonido. La presente revisión resume las diversas apariencias morfológicas de la patología renal y suprarrenal, muchas de las cuales exhiben características ultrasonográficas que permiten un diagnóstico veraz.

Acknowledgment

Andrew F. Little is a member of the Sisters of Charity Health Service.

References

1. Last, R.J.: Anatomy: Regional and Applied, 6th edition, Edinburgh, Churchill Livingstone, 1978, pp. 315–320
2. Yeh, H.C.: Sonography of the adrenal glands: normal glands and small masses. Am. J. Roentgenol. *135*:1167, 1980
3. Yeh, H.C., Mitty, H.A., Rose, J., Wolf, B.S., Gabrilove, J.L.: Ultrasonography of adrenal masses—unusual manifestations. Radiology *127*:475, 1978
4. Marchal, G., Gelin, J., Verbeken, E., Baert, A., Lauwerijns, J.: High resolution real time sonography of the adrenal glands: a routine examination? J. Ultrasound Med. *5*:65, 1986
5. Yeh, H.C.: Ultrasonography of the adrenals. Semin. Roentgenol. *23*:250, 1988
6. Gunther, R.W., Kelbel, C., Lenner, V.: Real time ultrasound of normal glands and small tumours. J. Clin. Ultrasound *12*:211, 1984
7. Tung, T.A., Pfister, R.C., Papanicolaou, N., Yoder, I.C.: Adrenal cysts: imaging and percutaneous aspiration. Radiology *173*:107, 1989
8. Murphy, B.J., Casillas, J., Yrizarry, J.M.: Traumatic adrenal hemorrhage: radiologic findings. Radiology *169*:701, 1988
9. Pery, M., Kaftori, J.K., Bar-Maor, J.A.: Sonography for diagnosis and follow up of adrenal haemorrhage. J. Clin. Ultrasound *9*:397, 1981
10. Vick, C.W., Zeman, R.K., Mannes, E., Cronan, J.J., Walsh, J.W.: Adrenal myelolipoma: CT and ultrasound findings. Urol. Radiol. *6*:7, 1984
11. Musante, F., Derchi, L.E., Zappasodi, F., Bazzocchi, M., Riviezzo, G.C., Banderali, A., Cicio, G.R.: Myelolipoma of the adrenal gland: sonographic and CT features. Am. J. Roentgenol. *151*:961, 1988
12. Bowerman, R.A., Sliver, T.M., Jaffee, M.H.: Sonography of adrenal phaeochromocytoma. Am. J. Roentgenol. *137*:1227, 1981
13. Hamper, U.M., Fishman, E.K., Harman, D.S., Roberts, J.L., Sanders, R.C.: Primary adreno-cortical carcinoma: sonographic evaluation with clinical and pathologic correlation in 26 patients. Am. J. Roentgenol. *148*:915, 1987
14. Vicks, B.S., Perusek, M., Johnson, J., Tio, F.: Primary adrenal lymphoma: CT and sonographic appearances. J. Clin. Ultrasound *15*:135, 1987
15. Paling, M.R., Williamson, B.R.: Adrenal involvement in non-Hodgkin's lymphoma. Am. J. Roentgenol. *141*:303, 1983
16. Dunnick, N.R., Korobkin, M., Frances, I.: Adrenal radiology: distinguishing benign from malignant adrenal masses. Am. J. Roentgenol. *167*:861, 1996
17. Forsythe, J.R., Gosink, B.B., Leopold, G.R.: Ultrasound in the evaluation of adrenal metastases. J. Clin. Ultrasound *5*:31, 1977
18. Cronan, J., Rosenfield, A.: Normal size of the adult kidney by real-time ultrasound. Am. J. Roentgenol. *154*:195, 1990
19. Emamian, S.A., Nielsen, M.B., Pedersen, J.F., Ytte, L.: Kidney dimensions at sonography: correlation with age, sex, and habitus in 665 adult volunteers. Am. J. Roentgenol. *160*:83, 1993

20. Hodson, J.: The lobar structure of the kidney. Br. J. Urol. *44*:246, 1972
21. Platt, J.F., Rubin, J.M., Bowerman, R.A., Maru, C.S.: The inability to detect kidney disease on the basis of echogenicity. Am. J. Roentgenol. *151*:317, 1988
22. Hederstrom, E., Forsberg, L.: Accuracy of repeated kidney size estimation by ultrasonography and urography in children. Acta Radiol. Diagn. *26*:603, 1985
23. Bozniak, M.A.: The current radiological approach to renal cysts. Radiology *158*:1, 1986
24. Hidalgo, H., Dunnick, N.R., Rosenberg, E.R., Ram, P.C., Korobkin, M.: Parapelvic cysts: appearance on CT and sonography. Am. J. Roentgenol. *138*:667, 1982
25. Sanders, R.C., Hartman, D.S.: The sonographic distinction between neonatal multicystic kidney and hydronephrosis. Radiology *151*:621, 1984
26. Taylor, A.J., Cohen, E.P., Erickson, S.J., Olson, D.L., Foley, W.D.: Renal imaging in long term dialysis patients: a comparison of CT and sonography. Am. J. Roentgenol. *153*:765, 1989
27. Choyke, P.L.: Inherited cystic diseases of the kidney. Radiol. Clin. North Am. *34*:925, 1996
28. Jennings, C.M., Gaines, P.A.: The abdominal manifestations of von Hippel-Lindau disease and a radiological screening protocol for an affected family. Clin. Radiol. *39*:363, 1988
29. Choyke, P.L., Glenn, G.M., Walther, M.M., Patronas, N.J., Linehan, W.M., Zbar, B.: Von Hippel-Lindau disease: genetic, clinical and imaging features. Radiology *194*:629, 1995
30. Mitnick, J.S., Bosniak, M.A., Hilton, S., Raghavendra, B.N., Subramanyam, B.R., Genieser, N.B.: Cystic renal disease in tuberous sclerosis. Radiology *147*:85, 1983
31. Rego, J.D., Laing, F.G., Jeffrey, R.B.: Ultrasonic diagnosis of medullary cystic disease. J. Ultrasound Med. *2*:433, 1983
32. Goiney, R.C., Goldenberg, L., Cooperberg, P.L., Charboneau, J.W., Rosenfield, A.T., Russin, L.D., McCarthy, S., Zeman, R.K., Gordon, P.B., Rowley, B.A.: Renal oncocytoma: sonographic analysis of 14 cases. Am. J. Roentgenol. *143*:1001, 1984
33. Bosniak, M.A., Megibow, A.J., Hulnick, D.H., Horii, S., Raghavendra, B.N.: CT diagnosis of renal angiomyolipoma: the importance of detecting small amounts of fat. Am. J. Roentgenol. *151*:497, 1988
34. Beckwith, J.B.: Multilocular renal cysts and cystic renal tumours. Am. J. Roentgenol. *136*:435, 1981
35. Charboneau, J.W., Hattery, R.R., Ernst, E.C., James, E.M., Williamson, B., Hartman, G.W.: Spectrum of sonographic findings in 125 renal masses other than benign simple cyst. Am. J. Roentgenol. *140*:87, 1983
36. Madayag, M.A., Ambos, M.A., Lefleur, R.S., Bosniak, M.A.: Involvement of the inferior vena cava in patients with renal cell carcinoma. Radiology *133*:321, 1979
37. Kler, R., Taylor, K.J., Feyock, A.L., Ramos, I.M.: Renal masses: characterization with Doppler US. Radiology *176*:703, 1990
38. Johnson, C.D., Dunnick, N.R., Cohen, R.H., Ilescas, F.F.: Renal adenocarcinoma: CT staging of 100 tumours. Am. J. Roentgenol. *148*:59, 1987
39. Leder, R.A., Dunnick, N.R.: Transitional cell carcinoma of the pelvicalices and ureter. Am. J. Roentgenol. *155*:713, 1990
40. Hartman, D.S., Davidson, A.J., Davis, C.J., Goldman, S.M.: Infiltrative renal and perirenal lymphoma: a further look. Clin. Radiol. *42*:233, 1990
41. Choyke, P.L., White, E.M., Zeman, R.K., Jaffe, M.J., Clarke, L.R.: Renal metastases: clinicopathologic and radiologic correlation. Radiology *162*:359, 1987
42. Rosenfield, A.T., Glickman, M.G., Taylor, K.J., Crade, M., Hodson, J.: Acute focal bacterial nephritis (acute lobar nephronia). Radiology *132*:553, 1979
43. Hoddick, W., Jeffrey, R.B., Golbberg, H.I., Federle, M.P., Laing, F.C.: CT and sonography of severe renal and perirenal infections. Am. J. Roentgenol. *140*:517, 1983
44. Hartman, D.S., Davis, C.J., Goldman, S.M.: Xanthogranulomatous pyelonephritis: sonographic-pathologic correlation of 16 cases. J. Ultrasound Med. *3*:481, 1984
45. Middleton, W.D., Dodds, W.J., Lawson, T.L., Foley, W.D.: Renal calculi: sensitivity for detection with US. Radiology *167*:239, 1988
46. Kamholtz, R.G., Cronan, J.J., Dorfman, G.S.: Obstruction and the minimally dilated renal collecting system: US evaluation. Radiology *170*:51, 1989